IRAQI JOURNAL OF APPLIED PHYSICS
Vol. 22, No. 2, April-June 2026, pp. 322-328

Synthesis, Characterization, and Photocatalytic Performance of CuO/TiO_2 Nanocomposite for Enhanced Methylene Blue Degradation

Aseel A. Auda [1*]
Firas K. Mohamad [2]

[1] Ministry of Education, Educational Directorate of Holy Kerbala, Kerbala, IRAQ
[2] Department of Physics, College of Science, University of Kerbala, Kerbala, IRAQ
Corresponding author email: aseeladnanalobaidi@gmail.com

In this work, an effective and low-cost CuO/TiO_2 binary metal oxide photocatalyst was synthesized via the polyol-mediated solvothermal route. The raw materials for the synthetic nanocomposite were titanium isopropoxide (TTIP) and copper (II) nitrate trihydrate. The structural and morphological properties of the framework substitution of CuO in the TiO_2 nanostructure were examined. The TiO_2 was crystallized in the tetragonal crystal structure as an anatase phase, doped with CuO nanoparticles after being calcined at 450°C for 3 hours. The one-dimensional CuO/TiO_2 structure was shown, forming as a rise-like structure. The BET-specific surface area of the CuO/TiO_2 nanocomposite was lower, but it had a larger pore size value compared to the undoped TiO_2. The results indicated that the degradation rate of the MB aqueous solution increased when pure TiO_2 was doped with CuO nanoparticles, reaching 99.80 % at 140 minutes of UV irradiation. The rate constants of the MB degradation reaction using pure TiO_2 and CuO/TiO_2 5 wt.% catalysts were 0.010 and 0.0184 min^{-1}, respectively.

Keyword: Nanocomposite; Polyol solvothermal; Copper oxide; Photodegradation
Received: 25 September 2025; Revised: 7 January 2026; Accepted: 14 January 2026; Published: 1 April 2026

1. Introduction

Transition inorganic metal oxides, including titanium dioxide (TiO_2) and cupric oxide (CuO), are a topic of sustained scientific interest to researchers. This interest stems from their probable applications in catalysis, sensors, optoelectronic instruments, cosmetics, biomedical field, and so on [1,2]. TiO_2 is an n-type semiconductor material with a broadband energy gap of roughly 3.2 eV. It is white in appearance. TiO_2 has several applications, such as paper, food, medical equipment coating, and gas sensors [3-5]. It has a significant advantage due to forming a heterojunction system when it reacts with another nanomaterial [5,6]. On the other hand, CuO is a semiconductor with a p-type conductivity and a small band gap of 1.2 eV. CuO has been utilized in numerous applications, such as nanocatalysis [7], batteries [8], magnetic devices [9], supercapacitors [10], etc.

The physical-chemical properties of TiO_2 and CuO depend on the obtained nanostructure, such as their size, morphology, and constituent grain orientations. Nanocomposites are created by combining one or more components to enhance and expand the applications of inorganic nanomaterials. The unique properties of such a nanocomposite are produced from their capacity to combine the best physical and chemical properties of their elements. One of these nanocomposites, the CuO/TiO_2 nanostructure, has garnered interest due to its small bandgap, non-toxicity, simple availability, and stability [11]. Various methods have been reported for the preparation of regular-sized two-oxide nanocomposites, including hydrothermal [12], sol-gel [13], chemical precipitation [14], solvothermal [15], and microwave-assisted [16], etc. Despite all the advances made, the preparation of TiO_2 nanoparticles and CuO/TiO_2 binary nanocomposite systems, which are dominated by shape and particle size, remains a significant challenge. The shape and size must be tailored by selecting suitable preparation conditions and methods. The precise control of the produced nano shape is of great significance since the particle surface energy, binding, the electronic properties of the nanostructure, and the chemical reaction of produced nanomaterials are immediately related to the obtained morphology of the surface [15].

In the present study, pure TiO_2 and CuO/TiO_2 binary metal oxide nanostructures were synthesized via a polyol-mediated solvothermal route. It investigated the effect of the CuO amount on the pristine TiO_2 surface nanoparticles and the morphology of the used precursor after calcination. This approach benefited from mixing the salt component at the nanoscale using ethylene glycol as a solvent. The photocatalytic properties of pure TiO_2 and TiO_2 doped with CuO nanoparticles were evaluated by the photodegradation of the organic dye methylene blue (MB).

2. Experimental Part

A polyol-mediated solvothermal process was used to synthesize pure TiO_2 nanoparticles. Typically, 100 mL of ethylene glycol solvent (EG, J.T. Baker 99.8% anhydrous solvent), $C_2H_4(OH)_2$ was heated to 170 °C

 © ALL RIGHTS RESERVED

using a hot plate and magnetic stirring. 2.5 mL of Titanium isopropoxide (TTIP, 98% Acros Organics) $C_{12}H_{28}O_4Ti$, was then added dropwise to the EG solution under constant stirring. A white-color titanium complex glycolate precipitate was obtained following the mixing process. The mixing process was maintained at a steady rpm for 5 hours. Then, the mix was left to cool down gradually to ambient temperature. The white precipitate was washed multiple times with an absolute ethanol (99.5% J.T. Baker Reagent), C_2H_5OH solution, and ultra-pure water to remove unwanted components. Finally, the white nanopowders were dried at 80 °C in a furnace for 6 hours and then calcined for 3 hours at 450 °C.

The CuO/TiO_2 nanocomposite oxide system was prepared using the same synthetic steps as mentioned before, except that when the white titanium glycolate was formed and cooled to 75 °C, 5 wt.% of Cupric (II) nitrate trihydrate (95%, J.T. Baker, Inorganic salt) $Cu(NO_3)_2.3H_2O$ as a doping agent precursor was added to the solution. A few drops of ammonium hydroxide solution (99.9%, J.T. Baker, basic), NH_4OH, were added until the pH value of the mixture reached 6. The obtained solution was reheated to 170 °C and stirred further for 1 hour at a constant rotation speed (rpm). Then, the light-blue precipitate was centrifuged and repeatedly cleaned with pure ethanol and ultrapure water. Finally, the prepared CuO/TiO_2 was dehydrated at 80 °C in an incubator for 8 hours and heat-treated at 450 °C for 3 hours.

The photocatalytic activity of bare TiO_2 and CuO/TiO_2 nanocomposite samples was evaluated by the photodegradation of methylene blue (MB, 99% Acros Organics), $C_{16}H_{18}CIN_3S$, in solution under UV irradiation with a source (wavelength approximately 365 nm, 16 W). 150 mg of catalyst was added to a glass beaker containing 500 mL of a 10 ppm MB dye solution. Before UV irradiation, the aqueous solution was stirred with a magnetic stirrer for 60 minutes in the dark to ensure the adsorption/desorption equilibrium of MB and the catalyst (pristine TiO_2 and CuO/TiO_2 5 wt.%). The initial concentration (C_0) of the MB and the concentration after irradiation time (C_t) were collected at 3 mL every 20 minutes. Then, the catalyst nanoparticles were separated from the dye solution by centrifuging at 4000 rpm for 5 minutes. The MB degradation was calculated using the formula: Degradation rate (%) = $(A_0\text{-}A)/A_0$, where A_0 and A were the absorbance of the primary and remaining MB dye, respectively.

To investigate the prepared crystalline structure and phase, an X-ray diffraction (XRD) technique (Aeris, Panalytical, Holland) was used. It was applied with Cu Kα irradiation at a wavelength of 0.154 nm, and the operation work (40 kV, 15-40 mA). The prepared specimens were scanned at 2θ angles from 5° to 90° with a step size of 0.05°/s to form the XRD patterns. The morphology of the obtained samples was examined using field-emission scanning electron microscopy (FE-SEM, Inspect F50, USA), which was coupled with an energy-dispersive X-ray (EDX) analyzer. The EDX technique was used to recognize the chemical elements in the tested sample matrix. The specific surface area of the synthesized samples was determined using a Brunauer-Emmett-Teller (BET) analyzer (Micromeritics ASAP 2010, GA, USA) with nitrogen gas adsorption-desorption analysis at 77 K. The absorbance value of MB in solution was measured using a UV/visible spectrophotometer (UV-VIS, Shimadzu, 1900i-Japan) in the wavelength range 190-1100 nm.

3. Results and Discussion

Figure (1) shows the XRD patterns of pure TiO_2 and CuO/TiO_2 5 wt.% nanocomposite system synthesized using the polyol-mediated solvothermal route and annealed at 450 °C for 3 hours. The results of the TiO_2 diffraction pattern showed that TiO_2 nanoparticles were present in the pure anatase crystal phase with lattice constants a = b = 3.75 Å, c = 9.53 Å, and angles α = β = γ = 90, as confirmed by JCPDS card 21-1272, which affirmed the formation of the TiO_2 nanostructure. No other diffraction peaks were observed in the pattern, indicating the high-purity phase of the titanium dioxide photocatalyst. XRD measurements revealed that the crystal planes (101), (004), (200), (105), (204), (220), (215), and (224) occur in the anatase TiO_2 nanoparticles, which correspond to angle diffraction (2θ) at 25.3°, 37.8°, 48.0°, 55.1°, 62.7°, 70.3, 75.1°, and 82.7° respectively.

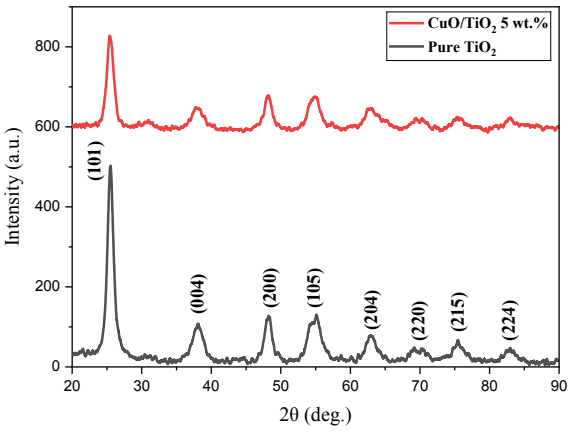

Fig. (1) XRD diffraction pattern of pure TiO_2 nanoparticles and CuO/TiO_2 5 wt.% nanocomposite

The CuO/TiO_2 5 wt.% nanocomposite system, as shown in Fig. (1), exhibited a pattern similar to that of pure anatase TiO_2 nanoparticles, without any additional diffraction peaks. The lattice parameters of the CuO/TiO_2 5 wt.% were calculated from the crystallographically planar (101), which found a = b = 3.79 Å, and c = 9.52 Å. This likely indicated the regular distribution of CuO nanoparticles in the pristine TiO_2 nanostructure. On the other hand, there are no peaks

 © ALL RIGHTS RESERVED

that belong to the CuO monoclinic phase in the XRD pattern, which can be due to a small amount of CuO dopant being used in this sample, and CuO peaks are too broad due to their small crystalline size [17]. The XRD results showed that the peak intensity was reduced and transformed into a broad peak as the TiO_2 nanoparticles were doped with CuO. This fact is due to the Ti^{4+} substitutional ions being replaced by Cu^{2+} dopant ions, which prevented the lattice nanostructure from distorting. The Debye-Scherrer equation was utilized to determine the average crystallite size (D) of the obtained nanostructure:

$$D = \frac{0.9\lambda}{\beta cos\theta} \quad (1)$$

where 0.9 is a constant known as shape factor, λ is the X-ray wavelength (0.154 nm), β is the full-width at half maximum (FWHM) of the diffraction peak, and θ is the diffraction angle [18]. The results show that the average crystallite size of pure TiO_2 and CuO/TiO_2 5 wt.% nanocomposite was about 7.50 nm and 6.44 nm, respectively. According to this finding, CuO loading inhibited particle growth because the Cu^{2+} ions on the TiO_2 structure combine to form a large nanoparticle.

The morphologies of pristine anatase TiO_2 and its doping with 5 wt.% CuO investigated by FE-SEM, as shown in Fig. (2). The results found that both bare TiO_2 and CuO/TiO_2 5 wt.% nanocomposite exhibited regular rise-like structures. The use of ethylene glycol (EG) as a solvent and a synthesis temperature of 170 °C were suitable conditions that contributed to the formation of this one-dimensional nanostructure. The increase in temperature and preparation time enhanced the hydrolysis formation rate, resulting in longer one-dimensional (1D) in this study [18]. The average length and diameter of the undoped TiO_2 rise-shaped structure were found to be approximately 3171.36 nm and 417.81 nm, respectively, as shown in Fig. (2a).

At 5 wt.% CuO loading, the morphology images showed a uniform TiO_2 rise-like structure, with CuO particles distributed on its surface. CuO and TiO_2 nanoparticles appeared as surface-phase junctions of the nanocomposite catalyst. These nanojunctions can promote the migration of interparticle carrier charges and facilitate the transport of photogenerated electrons from the TiO_2 conduction band (CB) to the CuO valence band (VB). Thus, the charge carrier (e^--h^+) separation efficiency and the photocatalytic activity are enhanced [19]. The CuO/TiO_2 5 wt.% had an average length and diameter of about 2448.95 nm and 385.09 nm, respectively. Table (1) summarized the average lengths and diameters of undoped TiO_2 and CuO/TiO_2 nanocomposite samples after being calcined at 450 °C for 3 hours.

Furthermore, the FE-SEM image showed that the CuO/TiO_2 5 wt.% nanocomposite was shorter and broader compared to the undoped TiO_2. When Cu^{2+} ions are incorporated into the TiO_2 structure, they partially substitute the ions of Ti^{4+} due to their similar ionic radius (Ti^{4+} = 0.68 Å and Cu^{2+} = 0.74 Å). However, the slightly large size of the ions Cu^{2+} produces local lattice distortions and creates internal strain within the TiO_2 structure. These local distributions create an undesirable environment for the unlimited growth of anatase TiO_2 rise-like structure [20-22].

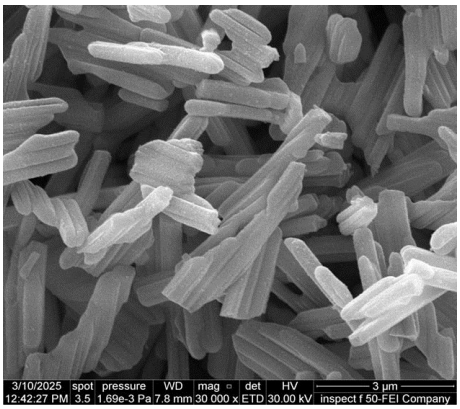

(a)

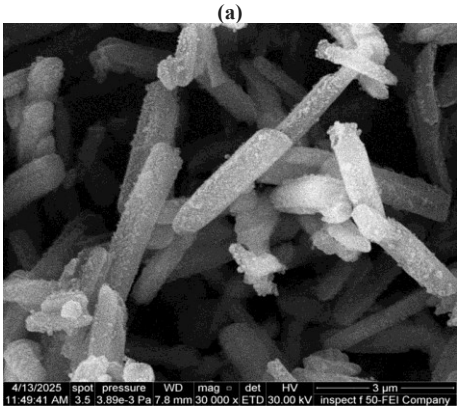

(b)

Fig. (2) FE-SEM images of (a) pure TiO_2 nanoparticles and (b) CuO/TiO_2 5 wt.% nanocomposite

Table (1) The average crystalline lengths and diameters of undoped TiO_2 and CuO/TiO_2 nanocomposite

Sample	Average length (nm)	Average diameter (nm)
Pure TiO_2	3171.36	417.81
CuO/TiO_2 0.5 wt.%	2448.95	385.09

Figure (3) shows the EDX results of undoped TiO_2 and CuO/TiO_2 5 wt.% nanocomposite, which explained the presence of peaks for titanium (Ti), oxygen (O), copper (Cu), and a small amount of impure carbon (C). The peak of C is attributed to the tape used to hold the tested sample during the measurement.

 © ALL RIGHTS RESERVED

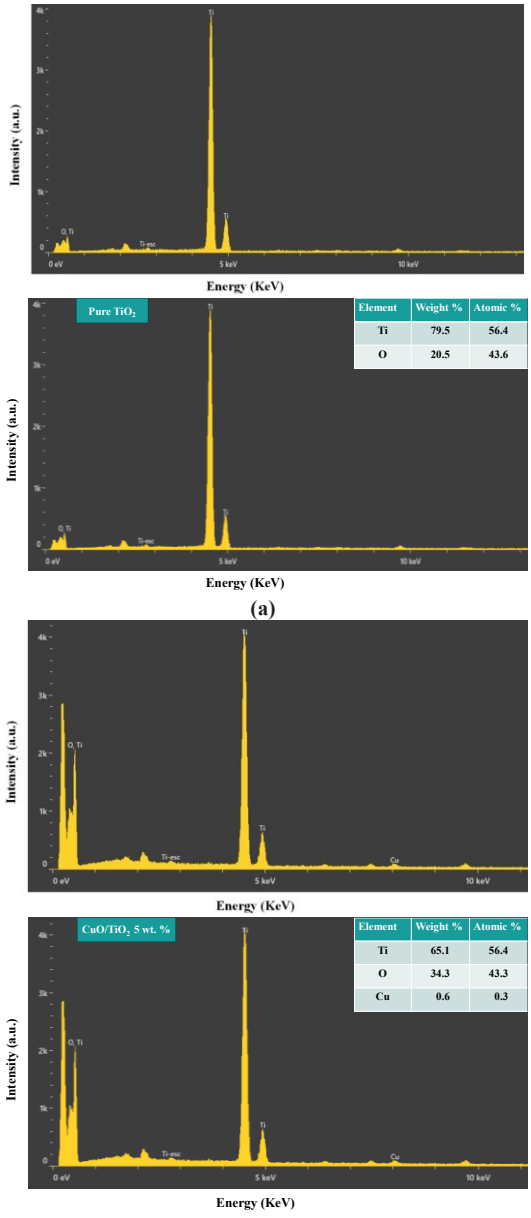

Fig. (3) EDX spectra of (a) undoped TiO_2 and (b) CuO/TiO_2 5 wt.% nanocomposite

To understand how the deposition of CuO nanoparticles affected the one-dimensional TiO_2 nanostructure of the created composite, the porous structure was analyzed using the nitrogen (N_2) adsorption-desorption isotherm. The BET result of the as-prepared undoped TiO_2 indicated a typical IUPAC kind IV pattern in the nitrogen gas isotherm, with the existence of an H3 type hysteresis loop, according to the BDDT classification [23], as shown in Fig. (4a). This kind of hysteresis loop implies the presence of irregularly sized and shaped slit-like pores. The specific surface area and average pore diameter of pure TiO_2 were 78.767 m^2/g and 7.504 nm, respectively. With doped TiO_2 by CuO nanoparticles at 5 wt.%, the BET finding revealed that an acquired isotherm with a hysteresis loop of the H1 type, as clarified in Fig. (4b). This result demonstrated the presence of regular cylindrical pores in the metal oxide system of the produced nanocomposites. The as-prepared CuO/TiO_2 5 wt.% nanocomposite had a specific surface area and average pore diameter of about 32.076 m^2/g and 8.534 nm, respectively. Table (2) displayed the BET of undoped TiO_2 and CuO/TiO_2 5 wt.% nanocomposite.

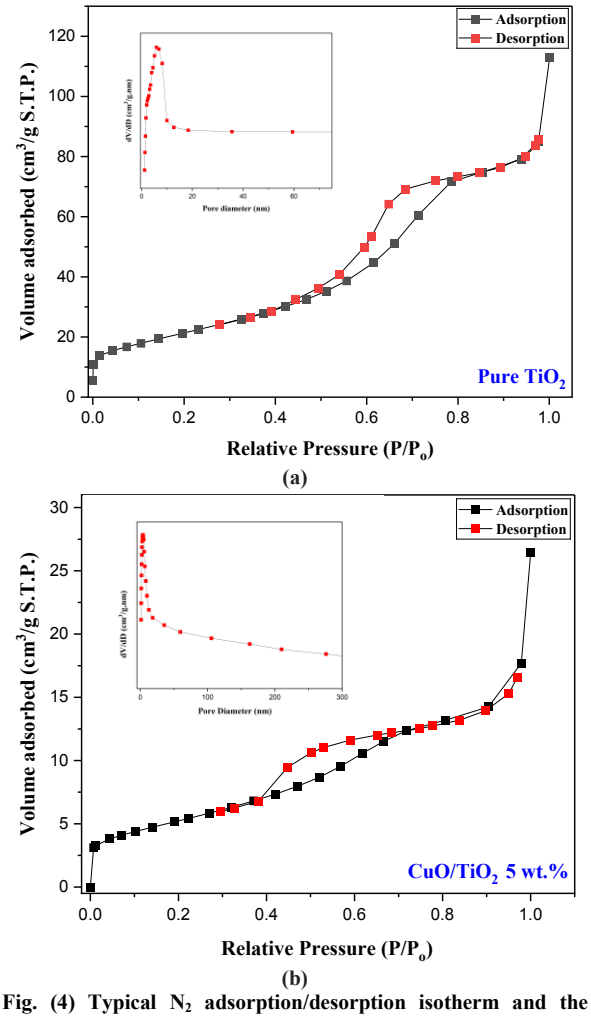

Fig. (4) Typical N_2 adsorption/desorption isotherm and the corresponding pore-size distribution curve (inset) of (a) pure TiO_2 and (b) CuO/TiO_2 5 wt.% nanocomposite

Table (2) Surface area and average pore diameter of pure TiO_2 and CuO/TiO_2 5 wt.% nanocomposite

Sample	Surface area (m^2/g)	Average pore diameter (nm)
Pure TiO_2	78.767	7.504
CuO/TiO_2 5 wt.%	32.076	8.534

From the BET results, the CuO/TiO_2 5 wt.% nanocomposite had a smaller surface area value but a higher pore diameter compared to the undoped TiO_2 nanostructure. This result may be due to the formation of CuO dopant and TiO_2 as a nanocomposite. According to IUPAC, the CuO/TiO_2 5 wt.% nanocomposite is considered a mesoporous material

 © ALL RIGHTS RESERVED

with pores that range in size from 2 to 50 nm [24]. The mesoporous structure of the photocatalyst facilitates the adsorption of reactants and the transfer of products, which enhances the photodegradation of organic pollutants. This feature made this sample potentially suitable for photocatalytic applications due to its well-developed porosity and well-formed crystalline structure. Therefore, the shape and type of pores are crucial for ensuring the efficiency and effectiveness of bare and nanocomposite photocatalysts in degrading pollutants, including dyes [25].

The photocatalytic activity of pure TiO_2 and the as-synthesized CuO/TiO_2 5 wt.% nanocomposite was investigated by observing the degradation of an MB solution under UV irradiation. The absorbance spectrum of MB degradation without prepared catalysts and with undoped TiO_2 and CuO/TiO_2 nanocomposite under UV irradiation was elucidated in Fig. (5). According to Fig. (5a), no degradation of the MB solution was observed in the absence of the prepared catalysts under UV irradiation for 180 minutes. The observed peak at 664 nm corresponded to the MB, which is responsible for the blue color of the MB solution. Further, this absorbed peak is used to observe the degree of degradation of the MB dye in an aqueous solution.

Under dark equilibration conditions for 60 min, the MB degradation of undoped TiO_2 and CuO/TiO_2 5 wt.% nanocomposite was approximately 5.1% and 9.9%, respectively. This indicated that the TiO_2 doped with CuO nanoparticles exhibited improved photodegradation abilities toward the MB solution. After a dark adsorption, the MB degradation of pure TiO_2 exhibited a considerable decrease in the intensity of the obtained peak at regular time intervals, from 20 to 180 minutes. The maximum MB photodegradation efficiency was approximately 93.57 % under UV irradiation. While the CuO/TiO_2 5 wt.% nanocomposite appeared effective for organic dye degradation, achieving approximately 99.80% degradation at 140 minutes of UV irradiation, as shown in Fig. (5c). This result was attributed to copper ions (Cu^{2+}) significantly enhancing the pristine TiO_2 photodegradation efficiency of MB dye. Furthermore, the low recombination rate of electron-hole (e^--h^+) pairs allows for additional interaction sites with MB molecules, resulting in high efficiency. Moreover, since both samples have a tiny crystalline size, the obtained peaks in the spectra were somewhat blue-shifted throughout the MB photodegradation process. The shafted peaks referred to an increase in the oxidation and reduction potentials of the charge carriers (electrons and holes). The rate of organic dye photodegradation was confirmed by the (e^--h^+) pairs with high oxidation-reduction power [26].

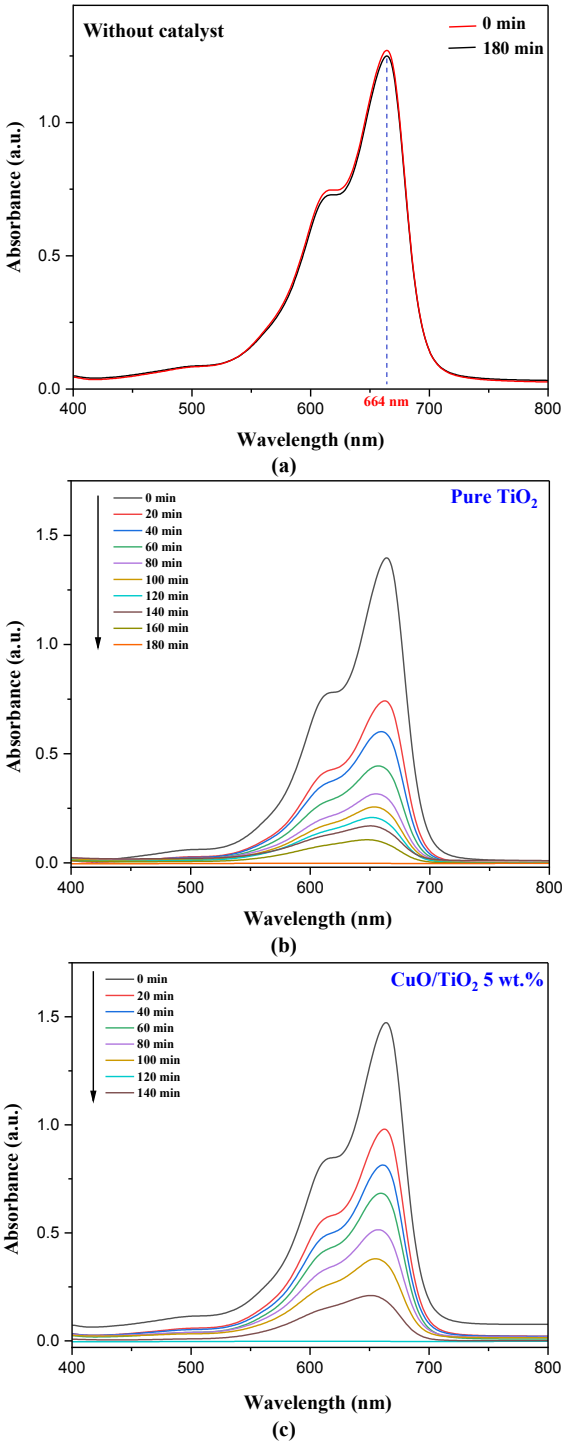

Fig. (5) Absorption spectra of the MB photodegradation (a) without catalysts, (b) using pure TiO_2, and (c) CuO/TiO_2 5 wt.% nanocomposite

The MB photodegradation was fitted to the Langmuir-Hinshelwood kinetics model. The slope of the value ln (C_0/C) plotted versus time of irradiation (min) indicated the value of the reaction rate constant (k) of the prepared catalyst, as shown in Fig. (6). Under UV irradiation, the photocatalytic performance was the highest value for the sample TiO_2 doped with CuO nanoparticles, with a rate constant of 0.0184 min^{-1},

 © ALL RIGHTS RESERVED

while that of pristine TiO_2 was shown at a kinetic rate constant of approximately 0.010 min^{-1}. The highest photocatalyst activity was attributed to the photo-generated electron (e) transfer from the conduction band (CB) of TiO_2 structure to CuO, which left a hole (h) in the TiO_2 lattice structure to participate in the oxidation reaction. That means the presence of CuO nanoparticles can reduce the electron-hole recombination rate in pure TiO_2. CuO particles deposited on the surface of the TiO_2 received the photo-generated electrons from the TiO_2 conduction band and formed copper ions (Cu^+). Then, Cu^+ ions can be reoxidized to Cu^{2+} by the reactive oxygen species (ROS) present in the surrounding medium [16,27].

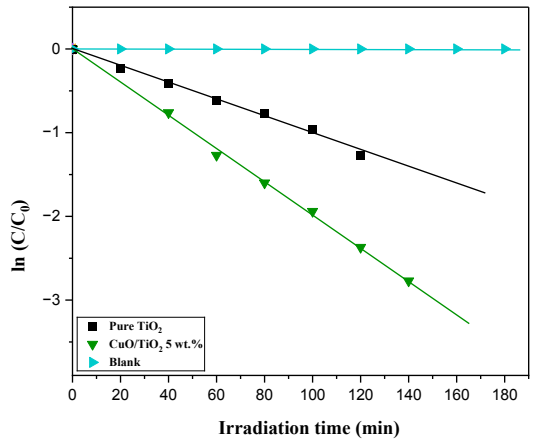

Fig. (6) First-order kinetics for the MB degradation on the pure TiO_2, CuO/TiO_2 5 wt.% nanocomposite, and without (blank) UV irradiation

Figure (7) explained the photocatalytic mechanism of the proposed pathway for the charge transfer approach in the CuO/TiO_2 nanocomposite. Under UV irradiation, both TiO_2 and CuO are excited and photogenerated electrons (e^-) from the conduction band (CB) of TiO_2 recombine with photogenerated holes (h^+) deriving from the conduction band (VB) of CuO, as shown in Eq. (2). This process led to the formation of more negative electrons and positive holes, which can occur directly between the two metal oxides due to the appropriate energetics of the relative positions of the TiO_2 conduction band and CuO valence band. The photoexcited (electrons and holes) could convert the MB aqueous molecules that were adsorbed on the surface of CuO/TiO_2 nanocomposite into hydrogen (H^+) and hydrogen ions (OH^-), as shown in Eq. (3). Hydroxyl radicals ($OH^•$) can be created when the adsorbed OH^- onions react with accumulating holes in the VB of CuO, as shown in Eq. (4). Superoxide radical ($O_2^•$) anion is created when concentrated electrons in the TiO_2 conduction band move to oxygen ($^-O_2$) atoms that have been adsorbed on the TiO_2 surface, as shown in Eq. (5). The oxygen atoms can also react with the H^+ cations to create an adsorbed hydroperoxyl radical (HO_2), which forms hydrogen peroxide (H_2O_2) when combined with electrons and H^+, as shown in equations (6-8). Moreover, a superoxide radical can combine with H_2O_2, reducing to hydroxyl radicals, as shown in Eq. (9). Predominantly, the degradation of a particular concentration of MB is controlled by the concentration of the produced $OH^•$ and $O_2^•$ radicals [28]. The photocatalytic mechanism of the CuO/TiO_2 nanocomposite was given in the following equations:

$$CuO/TiO_2 + h\nu \rightarrow CuO/TiO_2 + (e^- + h^+) \quad (2)$$

$$H_2O \leftrightarrow H^+ + OH^- \quad (3)$$

$$h^+ + OH^- \rightarrow OH^• + H^+ \quad \text{Oxidation} \quad (4)$$

$$e^- + O_2 \rightarrow O_2^{•-} \quad \text{Reductin} \quad (5)$$

$$O_2 + H^+ \rightarrow HO_2^• \quad (6)$$

$$H_2O + h^+ \rightarrow HO^• + H^+ \quad (7)$$

$$HO_2^• + e^- + H^+ \rightarrow H_2O_2 \quad (8)$$

$$H_2O + O_2^{•-} \rightarrow 2OH^• \quad (9)$$

The final products from the MB photodegradation are smaller molecules of carbon dioxide (CO_2) and water (H_2O) [29].

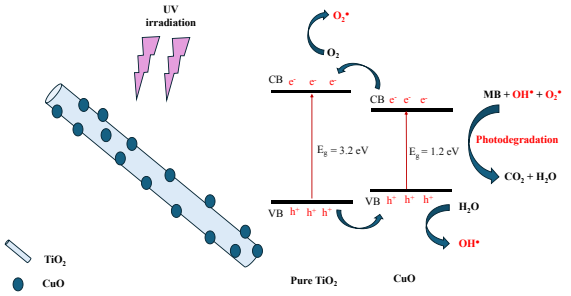

Fig. (7) Schematic diagram of the CuO/TiO_2 nanocomposite photocatalyst and photocatalytic mechanism of MB dye under UV irradiation

4. Conclusion

A simple process was used to prepare pure TiO_2 and a CuO/TiO_2 nanocomposite via a polyol-mediated solvothermal route. A synthetic solvent such as ethylene glycol (EG) was used to form a metal oxide system with a well-defined one-dimensional nanostructure. The results indicated that both samples showed a rise-like structure. The incorporation of CuO into TiO_2 nanostructure does not cause significant changes in the structure, possibly due to the substitution of Ti^{4+} ions with dopant Cu^{2+} ions. The CuO/TiO_2 nanocatalyst exhibited higher photocatalytic performance for the MB solution, achieving 99.80% degradation after 140 minutes of UV irradiation. The nanocomposite materials prepared in this work can be employed for various applications, including sensors, antimicrobial activity, and solar cell manufacture.

References

[1] M. Shah et al., "A new CuO/TiO_2 nanocomposite: an emerging and high energy efficient electrode material for aqueous asymmetric supercapacitors", *J. Ener. Storage,* 55 (2022) 105492.

 © ALL RIGHTS RESERVED

[2] P. Chudy et al., "Review of the development of copper oxides with titanium dioxide thin-film solar cells", *AIP Adv.,* 10(1) (2020) 010701.
[3] M. Gartner et al., "Advanced nanostructured coatings based on doped TiO_2 for various applications", *Molecules,* 28(23) (2023) 7828.
[4] J. Zhao et al., "The challenges and opportunities for TiO_2 nanostructures in gas sensing", *ACS Sensors,* 9(4) (2024) 1644-1655.
[5] S. Ghosh and A. Das, "Modified titanium oxide (TiO_2) nanocomposites and its array of applications: a review", *Toxicol. Environ. Chem.,* 97(5) (2015) 491-514.
[6] W. Wang et al., "Recent advances in TiO_2-based S-scheme heterojunction photocatalysts", *Chinese J. Catal.,* 55 (2023) 137-158.
[7] R. Nayak et al., "Fabrication of CuO nanoparticle: An efficient catalyst utilized for sensing and degradation of phenol", *J. Mater. Res. Technol.,* 9(5) (2020) 11045-11059.
[8] Y. Wang et al., "High specific energy of CuO as a thermal battery cathode", *Int. J. Electrochem. Sci.,* 15(10) (2020) 10406-10411.
[9] S. Atchaya and J. Meena Devi, "Experimental Investigation on Structural, Optical, Electrical and Magnetic Properties of Copper Oxide Nanoparticles", *Proc. Nation. Acad. Sci., India Sec. A: Phys. Sci.,* 94(1) (2024) 153-160.
[10] I. Bu and R. Huang, "Fabrication of CuO-decorated reduced graphene oxide nanosheets for supercapacitor applications", *Ceram. Int.,* 43(1) (2017) 45-50.
[11] H. Ashok, V. Rao and C. Chakra, "CuO/TiO_2 metal oxide nanocomposite synthesis via room temperature ionic liquid", *J. Nanomater. Mole. Nanotech.,* 5(2) (2016) 12-15.
[12] K. Manjunath et al., "Heterojunction $CuO-TiO_2$ nanocomposite synthesis for significant photocatalytic hydrogen production", *Mater. Res. Exp.,* 3(11) (2016) 115904.
[13] T. Ravishankar, M. Vaz and S. Teixeira, "The effects of surfactant in the sol-gel synthesis of CuO/TiO_2 nanocomposites on its photocatalytic activities under UV-visible and visible light illuminations", *New J. Chem.,* 44(5) (2020) 1888-1904.
[14] N. Ridha et al., "Synthesis and characterization of CuO nanoparticles and TiO_2/CuO nanocomposite and using them as photocatalysts", *AIP Conf. Proc.*, 2290 (1) (2020) 030006.
[15] J. Xia et al., "Ionic liquid-assisted hydrothermal synthesis of three-dimensional hierarchical CuO peachstone-like architectures", *Appl. Surf. Sci.,* 256(6) (2010) 1871-1877.
[16] S. Moniz and J. Tang, "Charge transfer and photocatalytic activity in CuO/TiO_2 nanoparticle heterojunctions synthesised through a rapid, one-pot, microwave solvothermal route", *Chem. Cat. Chem.,* 7(11) (2015) 1659-1667.
[17] T. Nguyen et al., "Synthesis and characterization of nano-CuO and CuO/TiO_2 photocatalysts", *Adv. Nat. Sci.: Nanosci. Nanotech.,* 4(2) (2013) 025002.
[18] M. Tulinski, "X-Ray Diffraction", in **Handbook of Nanomaterials for Hydrogen Storage**, Jenny Stanford Publishing (2017), pp. 79-101.
[19] P. Raizada et al., "Engineering nanostructures of CuO-based photocatalysts for water treatment: current progress and future challenges", *Arabian J. Chem.,* 13(11) (2020) 8424-8457.
[20] Y. Yu, Y. Chen and Z. Cheng, "Microwave-assisted synthesis of rod-like CuO/TiO_2 for high-efficiency photocatalytic hydrogen evolution", *Int. J. Hydro. Ener.,* 40(46) (2015) 15994-16000.
[21] D. Kumar et al., "CuO/TiO_2 nanocomposites: effect of calcination on photocatalytic hydrogen production", *J. Catal. Catal,* 1 (2014) 13-20.
[22] H. Guan et al., "Efficient and robust Cu/TiO_2 nanorod photocatalysts for simultaneous removal of Cr (VI) and methylene blue under solar light", *J. Chinese Chem. Soc.,* 65(6) (2018) 706-713.
[23] J. Yu and L. Shi, "One-pot hydrothermal synthesis and enhanced photocatalytic activity of trifluoroacetic acid modified TiO_2 hollow microspheres", *J. Mole. Catal. A: Chem.,* 326(1-2) (2010) 8-14.
[24] A. A'srai et al., "CuO/TiO_2 nanocomposite photocatalyst for efficient MO degradation", *Digest J. Nanomater. Biostruct.,* 18(3) (2023) 1005-1124.
[25] A. Haleem et al., "A comprehensive review on adsorption, photocatalytic and chemical degradation of dyes and nitro-compounds over different kinds of porous and composite materials", *Molecules,* 28(3) (2023) 1081.
[26] R. Rajput, S. Jamble and R. Bkale, "A review on TiO_2/SnO_2 heterostructures as a photocatalyst for the degradation of dyes and organic pollutants", *J. Environ. Manage.,* 307 (2022) 114533.
[27] M. Janczarek and E. Kowalska, "On the origin of enhanced photocatalytic activity of copper-modified titania in the oxidative reaction systems", *Catalysts,* 7(11) (2017) 317.
[28] P. Hajipour et al., "Surface modification of TiO_2 nanoparticles with CuO for visible-light antibacterial applications and photocatalytic degradation of antibiotics", *Ceram. Int.,* 47(23) (2021) 33875-33885.
[29] A. Bathla et al., "Morphology dependent photocatalytic activity of $CuO/CuO–TiO_2$ nanocatalyst for degradation of methyl orange under sunlight", *J. Nanosci. Nanotech.,* 20(5) (2020) 3123-3130.

 © ALL RIGHTS RESERVED